Astrophysics

Original article
UDC 524.6.
DOI: https://doi.org/10.18721/JPM.17313

INDIVIDUAL BEHAVIOR OF GAS HYDRODYNAMICS FROM PAIRS OF ISOLATED GALAXIES IN INTERACTION

E. Teófilo-Salvador ✉

National Autonomous University of Mexico, Mexico

✉ mca.ts.eduardo2015@gmail.com

Abstract. The hydrodynamic behavior of the gas of a selected pair of interacting galaxies has been reviewed based on numerical simulation using Illustris and IllustrisTNG. 210 halos were identified visually, using the Explorer; but their number was reduced due to selection taking into account found distances, masses and particle emission conditions, then the halos were refined and received specific cuts using Python. Among them, 34% did not interact at all, due to asymmetries ranging from 18 to 74%. The pair with ID 473420-473421 turned out to be the best interacting pair, and it was most marked at $z = 1$ and 5. This sample provided more information about the behavior of the gas present, such as the formation of tidal tails, with a relative velocity of 9 to 213 km/s. The density fields were affected by distribution velocities and radial motion in galaxy interaction processes, the gas flow created transitions between the two disks in the radial velocity field, with longer jets in regions of cold gas compared to those of hot one.

Keywords: ID 473420-473421, pair of isolated galaxies, numerical simulation

Funding: The author thanks the National Council of Humanities, Sciences and Technologies of Mexico, for the financial support for the postdoctoral stay 2021–2022 with numbers 930457 and 2420881 for 2022–2023, and to the ESTL-UAEH.

For citation: Teófilo-Salvador E., Individual behavior of gas hydrodynamics from pairs of isolated galaxies in interaction, St. Petersburg State Polytechnical University Journal. Physics and Mathematics. 17 (3) (2024) 148–160. DOI: https://doi.org/10.18721/JPM.17313

Научная статья
УДК 524.6
DOI: https://doi.org/10.18721/JPM.17313

ИЗУЧЕНИЕ ПАР ИЗОЛИРОВАННЫХ ВЗАИМОДЕЙСТВУЮЩИХ ГАЛАКТИК В АСПЕКТЕ ГИДРОДИНАМИЧЕСКОГО ПОВЕДЕНИЯ ГАЗА

Э. Теофило-Сальвадор ✉

Национальный автономный университет Мексики, г. Мехико, Мексика

✉ mca.ts.eduardo2015@gmail.com

Аннотация. В работе рассмотрено гидродинамическое поведение газа в выбранной паре изолированных галактик, основанное на численном моделировании Illustris и IllustrisTNG. Визуально в браузере Explorer было идентифицировано 210 ореолов, но их количество было уменьшено за счет выбора, учитывающего найденные расстояния, массы и условия выброса частиц; затем с помощью Python ореолы были доработаны и получили специфические разрезы. Среди них 34 % вообще не совершали взаимодействия ввиду наличия асимметрии (18 – 74%). Наилучшей взаимодействующей парой оказалась пара с идентификатором 473420-473421, причем она была лучше всего выражена при

значениях красного космологического смещения $z = 1$ и 5. Выбранная пара позволила получить больше информации о поведении присутствующего газа, например он проявляется в образовании приливных хвостов после взаимодействия с относительной скоростью от 9 до 213 км/с. На поля плотности влияют скорости распределения газов и их радиальное движение в процессах взаимодействия галактик; поток газа создает переходы между двумя дисками в поле радиальных скоростей, причем с более длинными струями в областях холодного газа, по сравнению с таковыми в горячих областях.

Ключевые слова: ID 473420-473421, пара изолированных галактик, численное моделирование

Финансирование. Автор благодарит Национальный совет Мексики по гуманитарным наукам, естественным наукам и технологиям за финансовую поддержку пребывания в докторантуре в 2021–2022 гг. (№№ 930457 и 2420881 от 2022–2023).

Для цитирования: Теофило-Сальвадор Э. Изучение пар изолированных взаимодействующих галактик в аспекте гидродинамического поведения газа // Научно-технические ведомости СПбГПУ. Физико-математические науки. 2024. Т. 17. № 3. С. 148–160. DOI: https://doi.org/10.18721/ JPM.17313

Introduction

The interaction of galaxies can occur as harassment, interaction, collision, fusion or cannibalism. Simulations have made it possible to describe these phenomena. The morphology and distribution of galaxy radial velocities are signs of recent interaction [1]. Gas-rich systems show star formation due to debris generated [2]. The presence of gas clouds and the density varies due to different coupling mechanisms such as intra clouds [3]. It was shown in Ref. [4] that cold gas inputted tend to smear the central metallicity of the galaxy, and M. Spavone et al. described in Ref. [5] that tidal encounters considerably removed the amount of mass from galaxies, and interaction and accretion mechanisms showed regions still being assembled. It was reported in Ref. [6] that gas mass flow altered the azimuth angle and became longer in directions aligned with the major and minor axes of the galaxies. Quantifying gas temperature, density, entropy, and cooling times is difficult, because entropy is sensitive to feedback energy injection, and is an indicator of gas cooling time [7].

Pairs of galaxies have been studied by many scientists. M. H. Hani et al. [8] analyzed 27,691 post-merger samples with $0 < z < 1$ (z is the cosmological redshift) uniformly distributed, obtaining star formation effects with redshift evolution. K. A. Blumenthal et al. [9] reported 446 pairs with $z = 0$, including star formation rate, galactic winds, metal enrichment, gas heating and cooling, black hole growth, and feedback. I. Wang et al. [10] applied CNN algorithms to report 6114 unique *R*-band galaxies with different orientations by classification into galaxy merger fractions.

R. Davé et al. [11] compared gas properties from the Simba, Eagle, and IllustrisTNG databases, based on cold interstellar gas modeling, with luminosity functions and gas mass ratios. These databases have been supported by codes for numerical simulations such as Enzo, Gadget, Flash, Athena, Ramses, Octo-Tiger, Gizmo or Arepo [12]. The Arepo code is more precise in the interactions between fast moving fluids and shocks such as gas, it ensures a better description due to mixing, of vorticity in curved shocks and a more efficient and realistic extraction of gas from the created substructures [13].

The simulations involve evolution over time and other elements; for example, the gas with dust is released more efficiently [14]. The condensation of metals in the gas phase forms dust grains that can reduce and induce a change in the cooling rate of the outer parts of the galaxy, this implies a change in active galactic nuclei, due to the change in the accretion rate [15]. J. S. Millard et al. [16] established that the evolution of the dust mass can generate a bias depending on the type of galaxies to be studied (satellite or central), leading to alterations in the surrounding gas.

The study of galaxy interaction has not been significant in statistical samples for large cosmological simulations [8], as even multiple physical processes can generate the same process asymmetry [17]. The behavior of the gas in the galactic interaction process is multicomponent, heterogeneous, irregular and discontinuous, due to morphology, propagation speed, travel speed, mass, density and distance, among other factors.

The goal of this research was to develop a simulation-based method for treating pairs of isolated galaxies interacting in the hydrodynamic gas behavior.

Methodology

Fig. 1 shows the methodological procedure designed to conduct the research.

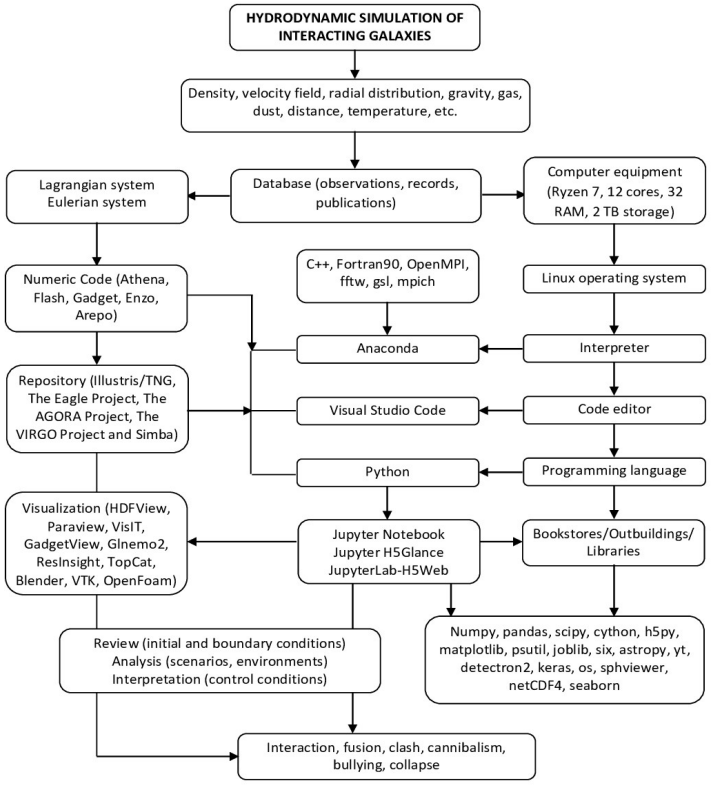

Fig. 1. Diagram of the methodology used (own elaboration)

Selection of galaxy pairs, processing and reduction. It started with the review of numerical codes [18]; an isolated galaxy was created with Enzo, Gadget-2 simulated a pair of interacting galaxies without the presence of gas and dust. To include the Arepo code approach, the IllustrisTNG database was used with 250 TB of data, including interactions ranging from 1 Gyr to less than 500 Myr [10]. Based on the Sublink merge tree methodology used in Ref. [8], in combination with the methodology used in Ref. [19], haloes were associated with their hosts and descendants, and at Jupyter-lab, haloes were identified with pairs of galaxies of similar masses, including interaction distance maxima.

For the visualization and interactive exploration of large data sets, such as those generated by simulations [20], the IllustrisTNG explore 2D and 3D interface was used, layers of different types of particles (gas, stars, dark matter and black holes) were superimposed. Free galaxies and satellite galaxies were taken into account, with massive haloes of 10^{12} $M_{\odot}$ and the case of not containing dark matter were considered purely stellar clusters [21]. At 400 kpc/h, through visual identification, 210 haloes with uniform interaction were recognized, at $z = 0$, under criteria of morphology, gas displacement, formation of bridges and tidal tails.

Identifying pairs in filaments was avoided due to the dense areas of gas and dust. Galaxies with the presence of gas and halos with low star formation were selected to obtain average

temperatures of the order of 104 K [7]. Similar to classification made in Ref. [9], each image was visually classified as interacting or not, based on the presence of a near neighbor, perturbed disks, and/or tidal features. Subsequently, the mass was reduced from 10^{12} to 10^{10} $M_{\odot}$.

Primary and secondary orbital motion was identified; with orbital decay, the pairs could interact or had interacted, so it was necessary to reduce the peripheral distance to 150 kpc. When considering the complete trajectories, samples that would not interact or that had had distant contact in the past were eliminated. To increase the reduction, it was inspected again and again, as some were in multiple subhaloes or were in the same group.

The sizes, distances, masses and their evolution over time were refined using Python. For the dataset of interest and the rendered images, 512 snapshots were generated and downloaded per galaxy, on average 19 GB per simulation review. The samples were no longer cut when central galaxies with satellites were detected, because they are not separated in the recorded observations [21].

The slices of interest were analyzed in Jupyter-lab and the snaps in Glnemo2 to identify interactive dynamic behavior, subsequently in VisIt and Paraview to detect variations or perceive attributes that were not observed in Glnemo2. The datasets and snapshots were also analyzed in HDFView.

Mechanics of pairs galaxies. The interaction speeds of $100 < V_{int} < 400$ km/s were discretized, with a similarity of masses and gas fraction greater than 20 %, in a high-velocity environment of almost frontal collision, and trajectories with traces of bridges or tails tidal [22].

In revising the interactions from $z = 0$ to $z = 10$, several pairs deconfigured the structures, causing a stretching of the field lines, and the vortex lines formed post-shock flows. These vortices were associated with tides, shear, and turbulence because they showed depletion and gas emissions [3, 23]. A normal, stationary alignment and a Mach number of 2 – 4 were needed for smooth interactions, which further reduced the initial samples. The post-shock wind was revised in prolonged interaction, generating a water hammer, the winds and jets aligned to generate a slowing of the flow patterns, this depended on the properties of the host galaxy.

Of the host galaxy, the circumgalactic neighborhood and the cosmic network were reviewed, the presence of disturbed or distorted filaments was tracked, to recognize the interaction force, such as the balance of forces of the tail or tidal bridges, defined as Q_{int} (with all masses as total mass [9]):

$$Q_{int} = \frac{F_{tidal} = \dfrac{M_n D_c}{R_{nc}^3}}{F_{bind} = \dfrac{M_c}{D_c^2}}, \tag{1}$$

where M_n is the mass of the neighboring galaxy; R_{nc} is the distance from the center of the galaxy to the neighboring one; M_c is the mass of the central galaxy; D_c is the diameter of the plant.

Under these criteria, the best pair that represented the interaction process was selected.

Hydrodynamics of the interacting gas. The equations of state and gravity were recognized, along with Poisson's equation, relaxation time, time to reach thermal equilibrium, and rate of energy change. The data sets were associated with the variables of the equations: conservation of mass, momentum and conservation of energy, which were of the following form:

$$\frac{\partial \rho}{\partial t} + \nabla \cdot (\rho \mathbf{u}) = 0, \tag{2a}$$

$$\left(\frac{\partial}{\partial t} + \mathbf{u} \cdot \nabla \right) u^i + \frac{1}{\rho} \partial_j P^{ij} = g^i, \tag{2b}$$

$$\frac{3}{2} \left(\frac{\partial}{\partial t} + \mathbf{u} \cdot \nabla \right) \frac{T}{m} + \frac{1}{\rho} P^{ij} \partial_i u_j + \frac{1}{\rho} \nabla \cdot \mathbf{q} = \frac{\dot{\varepsilon}}{m}, \tag{2c}$$

where $\mathbf{u}$ is the velocity of dark matter; P^{ij} is the pressure tensor; T is the temperature; $\mathbf{q}$ is the heat flux; ε is the local warming rate.

Moreover, the velocity dispersion was taken to be 1D (for simplicity) [24].

The exclusion of current interactions was imposed in advance, and in those cases where

the distribution of gas in and around a satellite galaxy was confused or perturbated [13]. When analyzing gas, IllustrisTNG was considered to overproduce cold gas in massive galaxies and molecular gas in small ones [11].

Results and discussion

Samples of galaxy pairs. As in Ref. [25], the selection of pairs was sensitive to the criteria and methods used. For data analysis, even training with CNN has shown 72 % accuracy between interactions and noninteractions [10], resulting in 28 % uncertainty. As in Ref. [9], in 34% of cases, there were errors in visual identification, due to vision, interpretation and visualization, the errors had the following sources:

i) finite resolution of the simulations;

ii) the stellar material was not the best indicator of a tail tidal force;

iii) the simulations instead of the observations;

iv) in very large impacts, the tidal forces were not strong enough to generate visible bridges or tails;

v) in cases of 1 Gyr the tide was partially noticeable, due to the evolution of the bridge or tail material that was deposited on the discs and could mix with the surrounding material.

The gas fraction ranged from 0.25 to 0.35, less than 10% of the paired samples contained no gas. The selected pairs had an asymmetry ranging from 18 to 74%, and only 26% reflected a symmetry being agree with that in Ref. [17]. A. B. Watts et al. described an asymmetry of more

Table 1

Positions and sizes of the pair of galaxies at different values of the redshift z

z	Position, *c*kpc/h			Size (particles)			
	x	*y*	*z*	Gas	Dark matter	Stars	Black holes
0.0	9796.38	31580.00	61031.80	111249	156742	32402	1
	9810.80	31577.40	61048.00	791	1724	12280	
0.5	51075.10	56805.90	41085.70	0	33	0	0
	51108.10	56944.60	40970.80		29		
1.0	63984.00	636.11	58526.30		30		
	64012.50	659.74	58565.70		29		
2.0	37898.40	42362.70	38639.50		23		
	22008.60	69636.30	14789.10	1932	7060	70	
3.0	24914.00	28079.20	36573.80	0	29	0	
	40989.50	34735.90	39956.60	992	1864	5	
4.0	3037.73	59471.70	64579.70	470	1388	8	
	3140.84	48911.40	63645.70	738	1089	5	
5.0	17824.60	47431.50	56736.60	15	21	0	
	17823.10	47399.80	56704.20	13	10		
6.0	40417.40	67385.70	35386.40	97	131	1	
	40401.40	67403.60	35880.20	44	112		
10	27507.70	54003.90	67587.70	38	44	0	
	28187.10	16769.50	53251.80	35	48	1	

Footnotes. 1. Here and in the other tables the data is presented for a pair of isolated interacting galaxies ID 473420-473421 (snapshots 99, 67, 50, 33, 25, 21, 17, 13 and 4). 2. For each value of *z* the numbers in the 1st and 2nd rows refer to galaxies ID 473420 and ID 473421, respectively.

Notation: *c*kpc/h is the comoving coordinate accepted in cosmology; where letter *c* means "comoving", kpc is kiloparsec, h is hour(s) in a cell, which is a spatial location within the periodic simulation domain of BoxSize.

Table 2

Masses, metallicity and star formation rates of the pair of galaxes at the redshift z

z	Mass, 10^{10} $M_\odot$/h					Gas metallicity M_z/M_{total}	Star formation rate, $M_\odot$/yr
	Gas	Dark matter	Stars	Black holes	Wind		
0.0	11.374700	79.244700	2.254370	0.003639	0.001651	0.017736	24.549200
	0.087954	0.871610	0.806995	0.004752		0.011294	0.338937
0.5	0	0.016684	0	0		0	0
		0.014662					
1.0	0	0.015167	0	0			
		0.014662					
2.0	0	0.011628	0	0			
	0.209526	3.569360	0.006044			0.001747	0.089967
3.0	0	0.014662	0	0		0	0
	0.111012	0.942391	0.000412		0	0.000568	0.009249
4.0	0.051526	0.701737	0.000869	0		0.001407	0.018829
	0.079690	0.550570	0.000429			0.000660	0.018412
5.0	0.001488	0.010617	0	0		0	0
	0.001333	0.005056					
6.0	0.010942	0.066230	0.000097	0			0.003665
	0.004793	0.056624	0.000117				0.001090
10	0.003587	0.022245	0	0			0.001684
	0.003486	0.024268	0.000128				0.001959

Notations: $M_\odot$/yr, $M_\odot$/h are the solar mass by year and by hour in the cell (see notation to Table 1); M_z/M_{total} is the ratio of the mass of all metals M_z to total mass.

than 40% within a virial radius, with morphologies reminiscent the hydrodynamic interaction of gases.

Dynamics of interaction simulation. The gas flow generated a transition strip in the radial velocity field, with a velocity distribution dispersing between the two disks and towards the center of the galaxies. In regions with cold gas, defined trails and filaments, longer, larger and redder tidal tails, were identified that differed in past interactions compared to recent ones.

In perpendicular encounters, an irregular distribution of masses was obtained, with the rotational movement of the most massive galaxy predominating. By removing the gas from the parallel interaction simulations, slightly inclined orbits were identified, with compensation for energy, density and velocity of the particles. Velocity followed curved or parabolic orbits, higher masses generated lower velocities and vice versa. This allowed us to differentiate a local maximum in its relative velocity (pericenter) and a minimum in each apocenter [9].

Mechanics in the specific sample simulation. The pair ID 473420-473421 was the one that best represented the interaction; its parameters are listed in Tables 1 − 4.

According to the tables data, there is interaction of the galaxy pair at z = 0.0, 0.5 and 1.0 (current era, 5.216 Gyr, 7.925 Gyr). At z = 2.0, 3.0 and 4.0 they move away (10.519, 11.658 and 12.263 Gyr). At z = 5.0 and 6.0 there is interaction (12.626 and 12.871 Gyr ago), and they separate at z = 10 (13.071 Gyr ago), see Fig. 2.

Table 3

Speed of the pair of galaxes at the redshift z

z	Speed, km/s					
	x	*y*	*z*	Maximum	Dispersal	Max radial
0.0	–9.9233	325.0820	–81.7149	213.7140	124.4350	30.3153
	69.5782	325.0830	–76.3504	126.2480	73.1109	3.1939
0.5	18.1919	236.0840	113.0530	9.3480	5.3219	9.9155
	–20.1042	370.8730	106.8270	11.4675	5.9947	6.2147
1.0	113.9510	–154.9760	–156.2260	13.3961	6.5835	5.3254
	64.8812	–89.2324	–235.2910	10.7468	5.3715	7.8986
2.0	–91.6826	–58.4907	75.3331	14.1931	7.9692	2.9171
	–324.7330	213.6400	–16.7254	79.9984	49.7336	57.7372
3.0	–81.3137	162.9840	305.3210	12.3979	6.9828	10.2084
	–100.1590	44.0363	–91.9193	54.9958	40.0558	39.2967
4.0	6.9603	–108.6070	–45.8049	61.7656	36.9068	28.9783
	18.3043	85.7583	–151.3030	51.4435	29.4478	33.5619
5.0	49.0199	–46.2195	–157.8860	12.4697	7.5701	8.5875
	62.9138	–41.1166	–153.0230	13.8873	7.7348	7.8690
6.0	–88.5341	–11.9263	188.1560	28.0516	17.0778	10.5887
	–98.9697	–37.7205	127.6330	31.9846	18.8272	13.9484
10	–186.4820	57.2344	–18.4205	27.9581	16.0782	12.6381
	19.9795	28.3001	–2.7225	27.7100	15.6528	12.4080

Table 4

The stellar photometry and spin of the pair of galaxes at the redshift z

z	Spin projection, (kpc/h)·(km/s)			Stellar photometry, mag		
	x	*y*	*z*	U	B	R
0.0	–291.0730	2942.2300	1143.6600	–22.6033	–22.1590	–22.4746
	–4.2051	83.4657	51.8481	–19.2736	–19.2736	–20.1710
0.5	0.4490	0.1847	–4.5583	0	0	0
	0.0693	5.6761	2.3837			
1.0	–0.6634	–2.3124	–1.3589	0	0	0
	5.6909	–6.5446	–0.5885			
2.0	–0.6987	0.8323	4.3076	0	0	0
	–147.6000	43.1684	–8.8838	–17.2910	–16.7648	–16.9979
3.0	–0.5921	–2.9726	–3.0945	0	0	0
	–84.5564	13.7292	–37.6379	–14.0718	–13.8110	–13.9165
4.0	–18.8156	–4.8045	66.8842	–15.3748	–15.0411	–15.1354
	34.2060	–0.4913	22.9933	–13.6737	–13.5620	–13.7512
5.0	0.4352	0.5800	–4.4037	0	0	0
	–2.4665	–0.7813	0.8567			
6.0	–1.7047	24.5405	–2.1670	–13.4396	–12.9881	–12.9330
	–1.0106	–2.3014	–2.7356	–12.6724	–12.4701	–12.5300
10	–0.1994	–1.6702	–0.8099	0	0	0
	0.3973	–2.3438	–0.0715	–15.0174	–13.6546	–13.5246

Footnotes. 1. Spin projections on the axes were computed for each as the weighted by mass sum of relative coordinates, multiplied by the relative velocity of all particles participating in the cell. 2. Mag units are taken as eight bands according to IllustrisTNG. Notations: U, B, R are ultraviolet, blue and red magnitudes.

The velocity pattern at z = 0.0, 1.0 and 5.0 was similar for both galaxies in the y and z directions, this reflected a more stable and balanced interaction. The maximum dispersion velocity was 124.35 and 73.11 km/s, respectively, for galaxies 473420 and 473421 at z = 0. The interaction resistance was very low of $\ln Q_{int}$ = 1.5 for masses close to 10^{12} and 2.5 for 10^{10}, so only the most distant ones contributed to a small tidal field. For the hydrodynamic analysis, greater precision was confirmed when analyzing the interaction part of the particles and subsequently analyzing the hydrodynamic part [11].

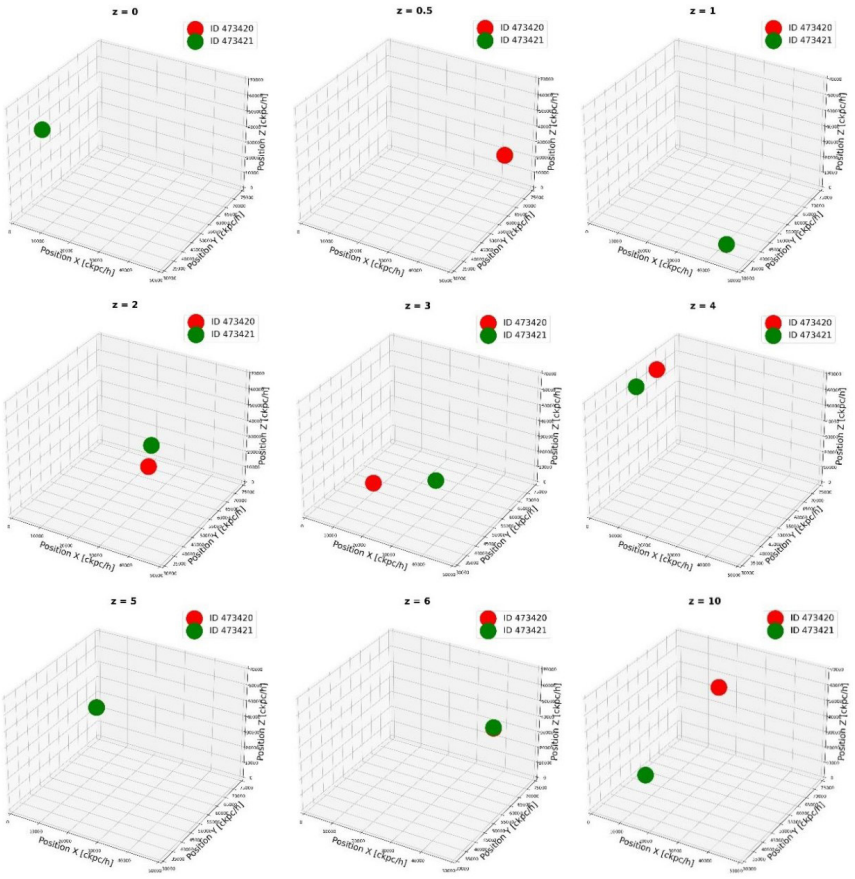

Fig. 2. Trajectory of snapshots 99, 67, 50, 33, 25, 21, 17, 13, 4 (own creation)

Gas hydrodynamics and the specific sample. Not all pairs contained gas, the halo finder did not associate gas particles despite the significant stellar masses. This represented 12 %, within the range of 7 % for Ref. [21]. Thus, gas averages were not appropriate for the interacting distributions [21]. Of the 300 snapshots examined, more than 60 % of the external gas had no effect on the internal one, the rebound caused changes in the relative speed, with small variations in angle and direction.

For the pair ID 473420-473421, the formation of tidal tails depended on the properties and geometry of the galaxies. The dominant metallicities produced massive star formation in the tidal tails, with strong interaction at z = 1 and 5. The specific relative velocity was from 9.34 to 213.71 km/s from 0 to 13.071 Gyr. High speeds separated the dark matter from the hot gas and compressed it by rebound, for the formation of star-like bodies, according to Ref. [22]. The interaction decreased towards low mass regions, due to distorted morphologies.

Galaxy 473421, with fewer particles and a smaller disk, was dominated by dark matter, generating similar rotation curves at z = 5. Heterogeneous, discontinuous and dispersed interactions were part of the evolution [13]. In Fig. 3, dramatic morphological transformations are observed, with deformation and distribution of gas in the galaxies, framed with rounded edges in each image.

Gas content showed no correlation with morphology. The gas fractions were very high and depended on the speed, mass and size of the galaxies.

In Fig. 3, the material was initially uncoupled and recoupled hydrodynamically and the winds removed the metal content of the mass, to keep it in equilibrium during the interaction. According to Ref. [9], the gas masses were ejected from the star-forming regions in the interactions, and the wind speed was proportional to the dispersion speed of the dark matter.

In the density fields, radial motion generated dense sweep, drag, and tidal tails, so gas coupling was strong. This led to the transfer of the thermal and ionization state of the evolved gas. Density increased with size, with dispersion speed not so great; in brighter regions the effect of gravity was greater, compared to the external pressure of the system. According to Ref. [8], this could lead to a substantial improvement in the density of the interacting gas. The interactions resulted in gas flows, created turbulence and could compress the gas. This process may be involved in the formation of new bodies. Like the possible formation of stars in areas with excess gas or denser gas, 2/3 of the central part of the galaxies is formed in this pair.

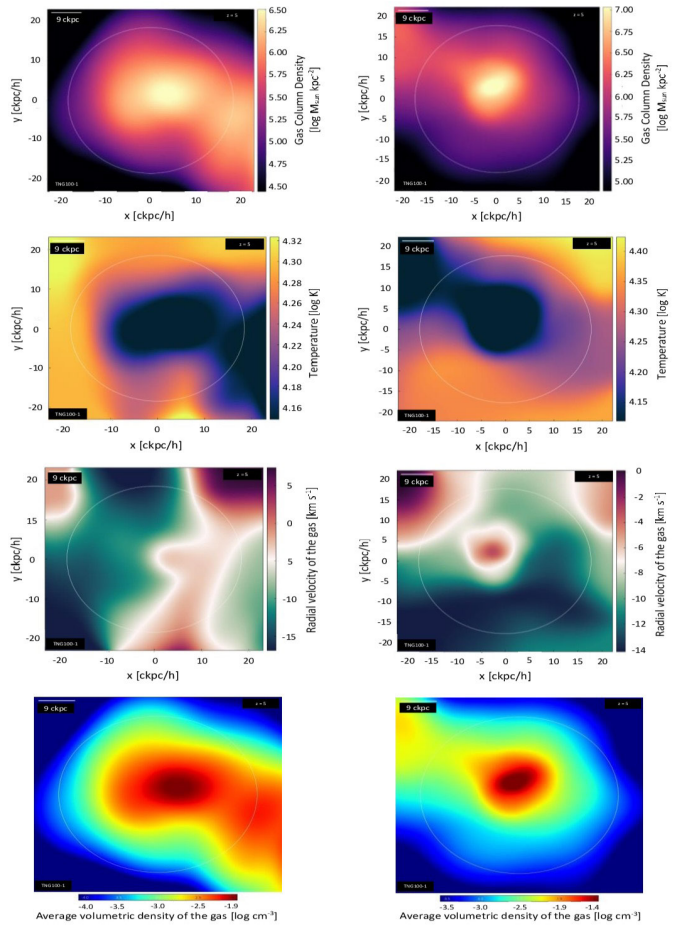

Fig. 3. Images of gas hydrodynamic parameters for a pair of interacting galaxies ID 473421 (left) and ID 473420 (right) based on simulation of TNG100-1 at $z = 5$. Parameters: cold gas density (1st row), gas temperature (2nd row), radial velocity (3rd row), volumetric density (4th row)

The gas entropy served as a good tool for diagnosing feedback (closed-loop) injection, because the gas was ejected by the shock which led to the emergence of wind with colossal kinetic energy not only due to the extinction of the masses, but also to the change in the thermodynamic properties of the gas elements itself, both inside galaxies and on their periphery. This affected ongoing star formation, with gas accreting up to several hundred kiloparsecs [7]. In terms of

massiveness, galaxy 473420 had a greater mass in the interaction process at $z = 1$ and 5, with little new gas which affected the kinetic feedback due to head-on collisions, with injection by sweeping and dragging of particles.

The gas metallicity was correlated with the radial velocity and flow direction along to the trajectories, as an indicator of the properties of the medium, the position and speed of the particles [6]. In interactions, the amount of gas participating in them exceeded the stellar mass, trajectory, density and temperature.

The hydrodynamic survey made it possible to trace the evolution before or after interaction, merger, contact or harassment, and the temporal influence of properties on galaxies, although the observations cannot trace the evolution due to the timing scheme. As in Ref. [19], the variety of tools and information provided by IllustrisTNG, made it possible to evaluate interactions, gas evolution and properties of galaxies (metallicity, morphology and star formation, orbital tracking).

Conclusions

Astrophysical and cosmological simulations require updated information, high-performance supercomputers and rigorous numerical codes for the analysis and interpretation of large data sets (gas, stars, black holes and dark matter), that, at different scales, shape the structure and evolution of the galaxies.

Of 210 samples of galaxy pairs, the visualization method presented disadvantages due to errors such as vision and interpretation of 34 %, less than 10 % did not present gas, and only 26 % reflected an interaction symmetry.

Of 300 snapshots, in more than 60 % the external gas did not influence the internal one, the interaction decreased towards low mass regions, due to distorted morphologies. The gas fractions depended on the speed, mass and size of the galaxies.

The pair that best represented the interaction evolution was ID 473420-473421 at $z = 0$, 1 and 5, where the distance between pairs of galaxies influenced the tidal tails, only at long distances was a relative degree of resistance to the interaction of 1.5 observed. The gas flow generated transitions in the radial velocity field between the two disks, with longer filaments in regions of cold gas compared to those of hot one.

The speed of the gases depended on their temperature and density, as well as on the rates of chemical reactions, which in turn depended on the rates of heating and cooling. These rates affected the interaction depending on the amount of added mass. In light interactions, bursts, weak flashes and short-lived asymmetries were observed, in interactions with a large amount of gas they were more prominent and lasting, until the system stabilized and the gas regrouped again, as shown in the pair ID 473420-473421.

Data availability

Related data is available at www.tng-project.org/, www.illustris-project.org/, https://www.youtube.com/@ingenieriacienciasbasicasy2477/videos

REFERENCES

1. **Fuentes-Carrera I., Amram P., Balkowski C., et al.,** Disentangling interacting galaxy pairs and entangling them back, ASP Conf. Ser. 390 (2008) 186–187.

2. **Paudel S., Duc P. A., Ree C. H.,** A case study for a tidal interaction between dwarf galaxies in UGC 6741, Astron. J. 149 (3) (2015) 114.

3. **Renaud F., Bournaud F., Agertz O., et al.,** A diversity of starburst-triggering mechanisms in interacting galaxies and their signatures in CO emission, Astron. Astrophys. 625 (13 May) (2019) A65.

4. **Zhang B-q., Cao Ch., Xu C. K., et al.,** The multi-object spectroscopy observation of seven interacting galaxy pairs: metallicity gradients and star formation distributions, Publ. Astron. Soc. Pac. 132 (1009) (2020) 034101.

5. **Spavone M., Iodice E., Capaccioli M., et al.,** VEGAS: A VST early-type galaxy survey. III. Mapping the galaxy structure, interactions, and intragroup light in the NGC 5018 group, Astrophys. J. 864 (2) (2018) 149.

6. **Péroux C., Nelson D., de Voort F., et al.,** Predictions for the angular dependence of the gas mass flow rate and metallicity in the circumgalactic medium, MNRAS. 2020. Vol. 499 (2, 21 Oct) (2020) 2462–2473.

7. **Zinger E., Pillepich A., Nelson D., et al.,** Ejective and preventative: The IllustrisTNG black hole feedback and its effects on the thermodynamics of the gas within and around galaxies, MNRAS. 499 (1, 10 Oct) (2020) 768–792.

8. **Hani M. H., Gosain H., Ellison S. L., et al.,** Interacting galaxies in the IllustrisTNG simulations – II: Star formation in the post-merge stage, MNRAS. 493 (3, 1 Apr) (2020) 3716–3731.

9. **Blumenthal K. A., Moreno J., Barnes J. E., et al.,** Galaxy interactions in IllustrisTNG-100, I: The power and limitations of visual identification, MNRAS. Monthly Notices of the Royal Astronomical Society. 492 (2, 1 Febr) (2020) 2075–2094.

10. **Wang I., Pearson W. J., Rodriguez-Gomez V.,** Towards a consistent framework of comparing galaxy merge in observations and simulations, Astron. Astrophys. 644 (03 Dec) (2020) A87.

11. **Davé R., Crain R. A., Stevens A. R. H., et al.,** Galaxy cold gas content in modern cosmological hydrodynamic simulations, MNRAS. 497 (1, 1 Sept) (2020) 146–166.

12. **Teófilo-Salvador E., Ambrocio-Cruz P., Rosado-Solis M.,** Methodological characterization and computational codes in the simulation of interacting galaxies, Artif. Intell. Appl. 2 (1) (2024) 45–58.

13. **Yun K., Pillepich A., Zinger E., et al.,** Jellyfish galaxies with the IllustrisTNG simulations: I. Gas-stripping phenomena in the full cosmological context, MNRAS. 483 (1, 11 Febr) (2019) 1042–1066.

14. **Armijos-Abendaco J., Lypez E., Llerena M., et al.,** Dust deficiency in the interacting galaxy NGC 3077, Galaxies. 5 (3) (2017) 53.

15. **Vogelsberger M., McKinnon R., O´Neil S., et al.,** Dust in and around galaxies: Dust in cluster environments and its impact on gas cooling, MNRAS. 487 (4, 21 Aug) (2019) 4870–4883.

16. **Millard J. S., B. Diemer D., Eales S. A., et al.,** IllustrisTNG and S2COSMOS: possible conflicts in the evolution of neutral gas and dust, MNRAS. Monthly Notices of the Royal Astronomical Society. 500 (1, 1 Jan) (2021) 871–888.

17. **Watts A.B., Power C., Catinella B., et al.,** Global HI asymmetries in IllustrisTNG: A diversity of physical processes disturb the cold gas in galaxies, MNRAS. 499 (4, 15 Oct) (2020) 5205–5219.

18. **Teófilo-Salvador E., Ambrocio-Cruz P., Rosado-Solis M.,** Introduction to Enzo for hydrodynamic simulations in astrophysics, Electron. J. Comput. Inform. Biomed. Electronic. (ReCIBE). 11 (2) (2022) C3-17.

19. **Patton D. R., Wilson K. D., Metrow C. J., et al.,** Interacting galaxies in the IllustrisTNG simulations – I: Triggered star formation in a cosmological context // arXiv: 2003.00289v2 [Astropphysics of Galaxies] Preprint 30 March 2020. Pp. 1–19. https://doi.org/10.48550/arXiv.2003.00289.

20. **Nelson D., Springel V., Pillepich A., et al.,** The IllustrisTNG simulations: Public data release, arXiv: 1812.05609v3[Astropphysics of Galaxies] for this version. 2021. (29 Jan) (2021) 1–30; https://doi.org/10.48550/arXiv.1812.05609.

21. **Diemer B., Stevens A. R. H., Lagos C. P., et al.,** Atomic and molecular gas in IllustrisTNG galaxies at low redshift, MNRAS. 2019. Vol. 487 (2, 1 Aug) 1529–1550.

22. **Shin E-J., Yung M., Kwon G., et al.,** Dark matter deficient galaxies produced via high-velocity galaxy collision in high-resolution numerical simulations, Astrophys. J. 899 (2) (2020) 25.

23. **Nolting C., Jones T. W., O´Neill B. J., Mendygral P. J.,** Interactions between radio galaxies and cluster shocks. I. Jet axes aligned with shock normal, Astrophys. J. 876 (2) (2019) 154.

24. **Famaey B., Khoury J., Penco R., A. Sharma A.,** Baryon-interacting dark matter: Heating dark matter and the emergence of galaxy scaling relations, J. Cosmolog. Astropart. Phys. 2020 (6) (2020) 025.

25. **Grylls P., Shankar F., Conselice C.,** The significant effects of stellar mass estimation on galaxy pair fractions, MNRAS. 99 (2, 1 Dec) (2020) 2265–2275.

СПИСОК ЛИТЕРАТУРЫ

1. **Fuentes-Carrera I., Amram P., Balkowski C., Flores H., Puech M., Yang Y., Rosado M., Hernбndez-Toledo H.** Disentangling interacting galaxy pairs and entangling them back // ASP Conference Series. 2008. Vol. 390. Pathways through an Eclectic Universe. Pp. 186–187.

2. **Paudel S., Duc P. A., Ree C. H.** A case study for a tidal interaction between dwarf galaxies in UGC 6741 // The Astronomical Journal. 2015. Vol. 149. No. 3. P. 114.

3. **Renaud F., Bournaud F., Agertz O., Kraljic K., Schinnerer E., Bolatto A., Daddi E., Hughes A.** A diversity of starburst-triggering mechanisms in interacting galaxies and their signatures in CO emission // Astronomy & Astrophysics. 2019. Vol. 625. 13 May. P. A65.

4. **Zhang B-q., Cao Ch., Xu C. K., Zhou Z-m., Wu Y.** The multi-object spectroscopy observation of seven interacting galaxy pairs: Metallicity gradients and star formation distributions // Publications of the Astronomical Society of the Pacific. 2020. Vol. 132. No. 1009. P. 034101.

5. **Spavone M., Iodice E., Capaccioli M., et al.** VEGAS: A VST early-type galaxy survey. III. Mapping the galaxy structure, interactions, and intragroup light in the NGC 5018 group // The Astrophysical Journal. 2018. Vol. 864. No. 2. P. 149.

6. **Péroux C., Nelson D., de Voort F., Pilleich A., Marinacci F., Vogelsberger M., Hernquist L.** Predictions for the angular dependence of the gas mass flow rate and metallicity in the circumgalactic medium // Monthly Notices of the Royal Astronomical Society. 2020. Vol. 499. No. 2. 21 October. Pp. 2462–2473.

7. **Zinger E., Pillepich A., Nelson D., Weinberger R., Pakmor R., Springel V., Hernquist L., Marinacci F., Vogelsberger M.** Ejective and preventative: The IllustrisTNG black hole feedback and its effects on the thermodynamics of the gas within and around galaxies // Monthly Notices of the Royal Astronomical Society. 2020. Vol. 499. No. 1. 10 October. Pp. 768–792.

8. **Hani M. H., Gosain H., Ellison S. L., Patton D. R., Torrey P.** Interacting galaxies in the IllustrisTNG simulations – II: Star formation in the post-merge stage // Monthly Notices of the Royal Astronomical Society. 2020. Vol. 493. No. 3. 1 April. Pp. 3716–3731.

9. **Blumenthal K. A., Moreno J., Barnes J. E., Hernquist L., Torrey P., Claytor Z., Rodriguez-Gomez V., Marinacci F., Vogelsberger M.** Galaxy interactions in IllustrisTNG-100, I: the power and limitations of visual identification // Monthly Notices of the Royal Astronomical Society. 2020. Vol. 492. No. 2. 1 February. Pp. 2075–2094.

10. **Wang I., Pearson W. J., Rodriguez-Gomez V.** Towards a consistent framework of comparing galaxy merge in observations and simulations // Astronomy & Astrophysics. 2020. Vol. 644. 03 December. P. A87.

11. **Davé R., Crain R. A., Stevens A. R. H., Narayanan D., Saintonge A., Catinella B., Cortese L.** Galaxy cold gas content in modern cosmological hydrodynamic simulations // Monthly Notices of the Royal Astronomical Society. 2020. Vol. 497. No. 1. 1 September. Pp. 146–166.

12. **Teófilo-Salvador E., Ambrocio-Cruz P., Rosado-Solis M.** Methodological characterization and computational codes in the simulation of interacting galaxies // Artificial Intelligence and Applications. 2024. Vol. 2. No. 1. Pp. 45 – 58.

13. **Yun K., Pillepich A., Zinger E., et al.** Jellyfish galaxies with the IllustrisTNG simulations: I. Gas-stripping phenomena in the full cosmological context // Monthly Notices of the Royal Astronomical Society. 2019. Vol. 483. No.1. 11 February. Pp. 1042–1066.

14. **Armijos-Abendaco J., Lypez E., Llerena M., Aldás F., Logan C.** Dust deficiency in the interacting galaxy NGC 3077 // Galaxies. 2017. Vol. 5. No. 3. P. 53.

15. **Vogelsberger M., McKinnon R., O´Neil S., Marinacci F., Torrey P., Kannan R.** Dust in and around galaxies: Dust in cluster environments and its impact on gas cooling// Monthly Notices of the Royal Astronomical Society. 2019. Vol. 487. No. 4. 21 August. Pp. 4870–4883.

16. **Millard J. S., B. Diemer D., Eales S. A., Gomez H. L., Beeston R., Smith M. W. L.** IllustrisTNG and S2COSMOS: possible conflicts in the evolution of neutral gas and dust// Monthly Notices of the Royal Astronomical Society. 2021. Vol. 500. No. 1. 1 January. Pp. 871–888.

17. **Watts A.B., Power C., Catinella B., Cortese L., Stevens A. R. H.** Global HI asymmetries in IllustrisTNG: a diversity of physical processes disturb the cold gas in galaxies // Monthly Notices of the Royal Astronomical Society. 2020. Vol. 499. No. 4. 15 October. Pp. 5205–5219.

18. **Teófilo-Salvador E., Ambrocio-Cruz P., Rosado-Solis M.** Introduction to enzo for hydrodynamic simulations in astrophysics // Computaciyn e Inform6tica [Computer Science & Informatics]. 2022. Vol. 11. No. 2. P. C3-17.

19. **Patton D. R., Wilson K. D., Metrow C. J., Ellison S. L., Torrey P., Brown W., Hani M. H., McAlpine S., Moreno J., Woo J.** Interacting galaxies in the IllustrisTNG simulations – I: Triggered star formation in a cosmological context // arXiv: 2003.00289v2 [Astropphysics of Galaxies] Preprint 30 March 2020. Pp. 1–19. https://doi.org/10.48550/arXiv.2003.00289.

20. **Nelson D., Springel V., Pillepich A. et al.** The IllustrisTNG simulations: Public data release // arXiv: 1812.05609v3[Astropphysics of Galaxies] for this version. 2021. 29 January. Pp. 1–30. https://doi.org/10.48550/arXiv.1812.05609.

21. **Diemer B., Stevens A. R. H., Lagos C. P., et al.** Atomic and molecular gas in IllustrisTNG galaxies at low redshift // Monthly Notices of the Royal Astronomical Society. 2019. Vol. 487. No. 2. 1 August. Pp. 1529–1550.

22. **Shin E-J., Yung M., Kwon G., Kim J-H., Lee J., Jo Y., Kiat O. B.** Dark matter deficient galaxies produced via high-velocity galaxy collision in high-resolution numerical simulations // The Astrophysical Journal. 2020. Vol. 899. No. 2. P. 25.

23. **Nolting C., Jones T. W., O´Neill B. J., Mendygral P. J.** Interactions between radio galaxies and cluster shocks. I. Jet axes aligned with shock normal // The Astrophysical Journal. 2019. Vol. 876. No. 2. P. 154.

24. **Famaey B., Khoury J., Penco R., A. Sharma A.** Baryon-interacting dark matter: Heating dark matter and the emergence of galaxy scaling relations // Journal of Cosmology and Astroparticle Physics. 2020. Vol. 2020. No. 6. P. 025.

25. **Grylls P., Shankar F., Conselice C.** The significant effects of stellar mass estimation on galaxy pair fractions // Monthly Notices of the Royal Astronomical Society. 2020. Vol. 499. No. 2. 1 December. Pp. 2265–2275.2001.06017.

THE AUTHOR

TEÓFILO-SALVADOR Eduardo
National Autonomous University of Mexico (UNAM)
National School of Earth Sciences-UNAM
Scientific Research S/N, C. U., 04510, México
mca.ts.eduardo2015@gmail.com
ORCID: 0000-0001-8794-2938

СВЕДЕНИЯ ОБ АВТОРЕ

ТЕОФИЛО-САЛЬВАДОР Эдуардо – *PhD (науки о Земле), профессор Национального автономного университета Мексики (UNAM), профессор Национальной школы наук о Земле, UNAM; г. Мехико, Мексика.*
Scientific Research S/N, C. U., 04510, México
mca.ts.eduardo2015@gmail.com
ORCID: 0000-0001-8794-2938

Received 04.01.2024. Approved after reviewing 17.04.2024. Accepted 17.04.2024.
Статья поступила в редакцию 04.01.2024. Одобрена после рецензирования 17.04.2024. Принята 17.04.2024.